Mater. Res. Soc. Symp. Proc. Vol. 1208 © 2010 Materials Research Society 1208-O10-02

Effect of Size, Shape, Composition, and Support Film on Localized Surface Plasmon Resonance Frequency: A Single Particle Approach Applied to Silver Bipyramids and Gold and Silver Nanocubes

Emilie Ringe[1], Jian Zhang[1], Mark R. Langille[1], Kwonnam Sohn[2], Claire Cobley[3], Leslie Au[3], Younan Xia[3], Chad A. Mirkin[1], Jiaxing Huang[2], Laurence D. Marks[2] and Richard P. Van Duyne[1]
[1]Chemistry, Northwestern University, Evanston, Illinois; [2]Materials Science and Engineering, Northwestern University, Evanston, Illinois; [3]Biomedical Engineering, Washington University, St. Louis, Missouri.

ABSTRACT

Localized surface plasmon resonances (LSPR), collective electron oscillations in nanoparticles, are being heavily scrutinized for applications in chemical and biological sensing, as well as in prototype nanophotonic devices. This phenomenon exhibits an acute dependence on the particle's size, shape, composition, and environment. The detailed characterization of the structure-function relationship of nanoparticles is obscured by ensemble averaging. Consequently, single-particle data must be obtained to extract useful information from polydisperse reaction mixtures. Recently, a correlated high resolution transmission electron microscopy (HRTEM) LSPR technique has been developed and applied to silver nanocubes. We report here a second generation of experiments using this correlation technique, in which statistical analysis is performed on a large number of single particles. The LSPR dependence on size, shape, material, and environment was probed using silver right bipyramids, silver cubes, and gold cubes. It was found that the slope of the dependence of LSPR peak on size for silver bipyramids increases as the edges become sharper. Also, a plasmon shift of 96 nm was observed between similar silver and gold cubes, while a shift of 26 nm was observed, for gold cubes, between substrates of refractive index (RI) of 1.5 and 2.05.

INTRODUCTION

The plasmonic properties of nanoparticles have attracted much attention in the past decade. Their potential use in sensing devices[1, 2], waveguides[3, 4], and photonic circuits[5-7] makes them a very active area of research. The localized surface plasmon resonance (LSPR) of such nanoparticles lies at the heart of such applications. Localized surface plasmons occur when the electrons in the particle interact with electromagnetic radiation, leading to selective photon absorption and radiation, as well as enhanced electromagnetic fields around the particle. The latter property is heavily used in surface-enhanced Raman spectroscopy (SERS)[8], while the former gives rise to bright colors, leading to their use in stained glass. Understanding plasmonic properties is essential to produce optimized devices, yet the current knowledge on this subject is mostly derived from experiments performed at the ensemble-averaged level on nanoparticle solutions. While such data can be useful, for example in giving trends related to dependence on LSPR on material, shape, size, and environment, conclusions drawn using heterogeneous mixtures are limited by the solution composition, which is usually less than perfect. To resolve this ensemble-averaging issue, researchers have turned to single-particle experiments. Systematic analyses using correlated structural and optical characterization have only emerged very recently [9-11], and much more can be learned from rigorous single particle analysis of the factors

dictating the plasmonic properties of metal nanoparticles. In this study, we use single particle measurements to examine the effects of size, substrate dielectric properties, composition and shape on the plasmonic properties of cubes and bipyramids.

EXPERIMENTAL DETAILS

Silver bipyramids were synthesized using a plasmon-mediated technique previously published[12]. Single crystalline Ag cubes were synthesized using previously reported polyol methods[13]. Gold nanocubes were prepared following a published procedure[14]. Three different types of grids were used in this study. Ultrathin carbon type A and carbon type B grids, copper grids coated with Formvar (30 to 60 nm) and a layer of amorphous carbon (A: 3-4nm, B: 15-25nm), were obtained from Ted Pella Inc. Silicon nitride grids of approximate stoichiometry Si_3N_4, in which the support film is 100 nm thick, were obtained from SPI Supplies Inc.

A 1-5µL drop of an aqueous suspension of nanoparticles was put on the support film, and dried in air. For carbon type A and B grids, the particles were deposited such that they were in direct contact with the Formvar. Dark field scattering was used to obtain LSPR spectra, following a previously reported procedure[11], summarized in Figure 1. TEM images were obtained within days of the optical characterization on either a JEOL JEM2100 FAST TEM or a Hitachi HD-2300A STEM, both operated at 200kV.

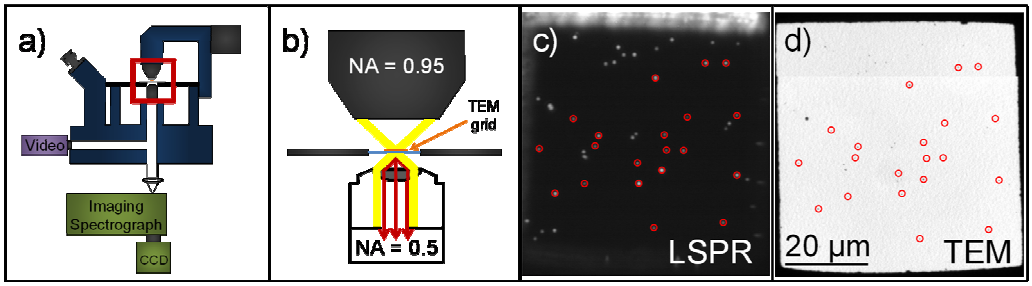

Figure 1. Experimental details of correlated LSPR/TEM measurements: a) inverted optical microscope, b) dark field condenser, sample, and collection objective, c) dark field Rayleigh scattering image of a grid square, d) low magnification TEM image of the same grid square.

RESULTS AND DISCUSSION

Gold and silver nanocubes

Gold and silver nanocubes were synthesized and analyzed using correlated HRETM-LSPR. The effects of a substrate, unlike those of homogeneous dielectric environment, on LSPR have rarely been studied systematically in the past[15], despite the potential for advancement of enhancing surfaces such knowledge offers. To probe this effect at the single particle level, gold cubes were deposited on silicon nitride (RI: approx. 2.05) and carbon type B grids (Formvar side, RI:1.475[16]). Additionally, the dependence of the LSPR on the composition of the cubes was investigated by comparing gold and silver cubes deposited on identical substrates. A typical LSPR spectrum for a single gold nanocube on a Formvar film is presented in Figure 2. LSPR spectra on Si_3N_4 are similar, thus omitted for clarity. The small peak around 440 nm is due to interband transitions from the d to sp band. The main feature in the spectrum, in the 550-650 nm

region, is due to dipolar resonances. Figure 2 also shows a typical LSPR spectrum for a silver cube on a Formvar substrate. The sharp peak at 405 nm is attributed to a quadrupole mode, while the peak at 484 nm is attributed to the dipolar resonance [10, 17]. Calculations are currently underway to explain the absence of the sharp blue peak from the gold cubes spectra.

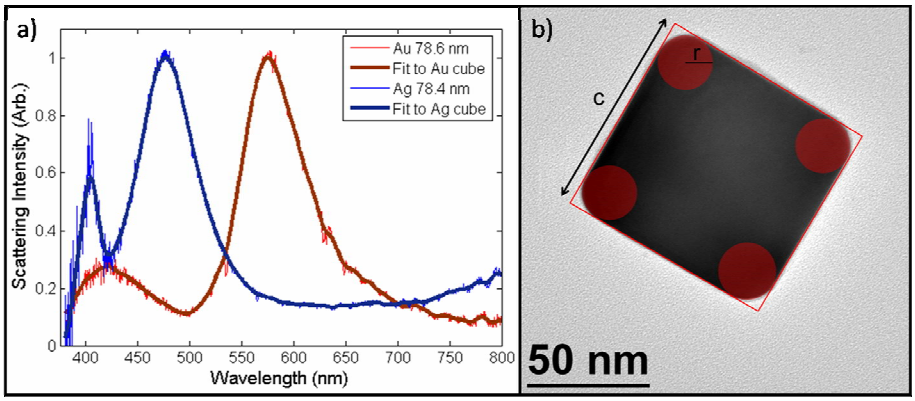

Figure 2. Correlated HRETM-LSPR of Au and Ag cubes on Formvar: a) Typical LSPR spectra for a 78.6 nm gold cube and a 78.4 nm silver cube, b) silver nanocube showing measurements used: c is the face-to-face distance (size), and r is the radius of curvature for the corner rounding.

From the data acquired using correlated HRETM-LSPR, only single cubes presenting straight edges, an aspect ratio between 0.95 and 1.05, and a radius of curvature average of less than 22 percent of the face to face distance were used, yielding 54, 24, and 12 data points for silver cubes on Formvar, gold cubes on Formvar, and gold cubes on silicon nitride, respectively. The aspect ratio condition arises from the fact that nanorods display two dipolar resonances (transverse and longitudinal) instead of one, which would affect the results by shifting the observed LSPR maximum to the blue or to the red, depending on which mode is more strongly excited. The radius of curvature also influences the position of the wavelength of the LSPR maximum [10]. Detailed calculations on this effect are in progress[18].

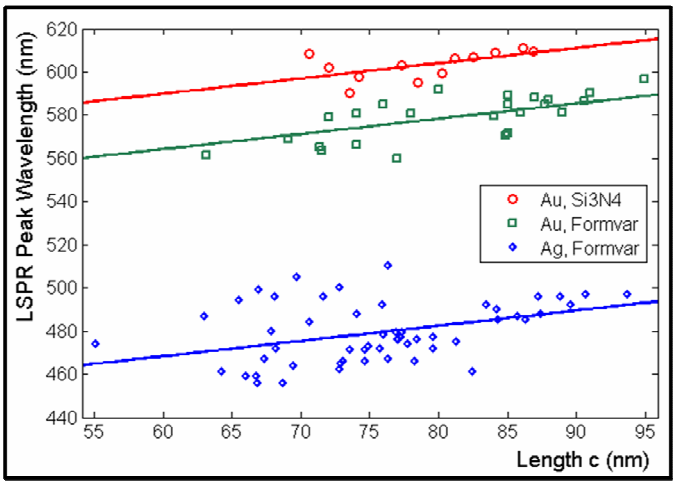

Figure 3. Effect of composition and substrate dielectric properties on the dipolar plasmon of metal nanocubes. The difference in LSPR peak for gold cubes on Formvar (RI: 1.475) and Si_3N_4 (RI 2.05) is 26 nm. This difference is 96 nm between silver and gold cubes on identical films.

The dependence of LSPR peak on the size and composition of the cube, as well as on the substrate refractive index is presented in Figure 3. The LSPR maximum varies linearly in this region, although a theoretical exponential dependence has been suggested over a larger range[19]. The effect of the substrate is a marked shift of the plasmon resonance: from Formvar (RI:1.475) to silicon nitride (RI: 2.05), the LSPR maximum shifts by 26 nm. Holding all other factors constants, changing the composition from Au to Ag shifts of the dipolar resonance by 96 nm. The slopes of the plasmon resonance increase as a function of size was found not to be significantly different for the three data sets by analysis of covariance (ANCOVA, p=0.63), hence a second ANCOVA model was used to find the slope (0.706) and intercepts of the parallel lines.

Silver bipyramids

Silver right bipyramids were chosen to study the effect of corner rounding on optical properties because, unlike rather homogeneous cubes, a large range of rounding can be found in any given solution. Such structures are related to cubes by the fact that they both present (100) faces and 90˚ angles. The bipyramidal shape also has a (111) twin plane at its center, yielding a structure akin to two cube apexes joined together[12, 20]. On a substrate, the bipyramids lay on one of their six identical faces, which give rise to a two dimensional projection as in Figure 4c. The sizes used through this analysis are the untruncated length of a, which represents the edge length of the equilateral triangle defined by the (111) twin plane, while the truncation reported is the height of a triangle fitting in the empty region defined by the "perfect" bipyramid overlay (see Figure 4). Relative rounding was computed as the truncation length over the length a.

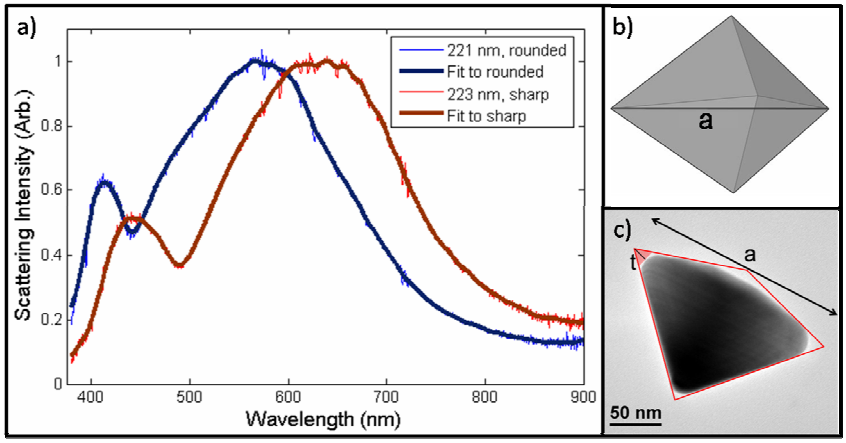

Figure 4. Correlated LSPR/TEM of silver bipyramids on Formvar: a) LSPR spectra for bipyramids of similar size and different rounding, b) 3D model of a right bipyramid showing a as the equilateral base triangle edge length, c) bipyramid measurements, where the truncation length t is the height of a triangle fitting in the empty space formed by the ideal bipyramid drawing.

Bipyramids from four different reaction mixtures were used. The analyzed bipyramids produced by illumination of silver seeds with 500±20, 550±20, 600±20, and 650±20 nm light had an average size of 160, 203, 228, and 239 nm, respectively. LSPR spectra were obtained from single bipyramids on the Formvar side of carbon type B grids. Typical spectra are presented

in Figure 4. The peak around 420 nm has been attributed, on the basis of DDA calculations[12], to the transverse resonance, i.e. the resonance between the two 90˚ angles at the top of each pyramid. Experiments are currently underway to confirm this assignment. The peak around 600 nm arises from the longitudinal resonance, i.e. a plasmon parallel to the (111) twin plane. Previous calculations stress the sensitivity of this peak to the rounding of the equatorial corners[12]. In this work, rounding is shown to not only shift the plasmon resonance for a given shape, but also to change the dependence of the plasmon peak on the size of the particle.

The dipolar plasmon peak dependence on size and truncation for bipyramids is presented in Figure 5. The bipyramids were divided into three relative rounding categories: sharp (5 to 8%), average (8 to 9.5%) and round (9.5 to 12%). The slope of the size dependence of the LSPR maximum is 1.07(0.07) and 0.58(0.07) for sharp and rounded particles, respectively. The slope of the average bipyramids falls between the slope of the sharp and rounded (data not shown). The difference between the sharp and rounded slopes is statistically significant, as confirmed by an analysis of covariance (p=0.0006). The implication of this result is that the more anisotropic a bipyramid is, the more sensitive it is to a size change. This property can be extremely useful when tailoring the plasmon of enhancing surfaces.

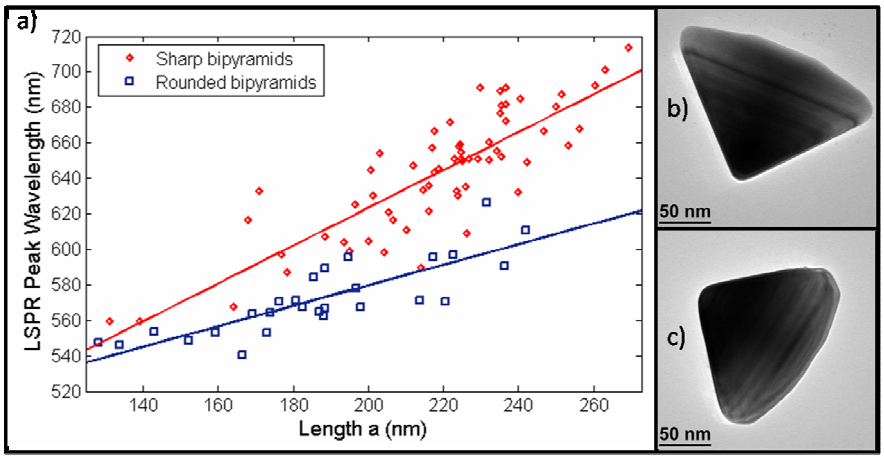

Figure 5. Effect of corner rounding and size on the dipolar plasmon silver bipyramids: a) Plot of the LSPR maximum as a function of size for two groups of rounding. The slopes, 1.07(0.07) for sharp particles and 0.558(0.07) for rounded ones, are significantly different b) example of a particle from the sharp group, c) example of a particle from the rounded group.

CONCLUSIONS

By using Correlated HRETM-LSPR on single nanoparticles, it was possible to probe the effect of size, shape, composition, and substrate refractive index on the plasmonic properties of silver right bipyramids and nanocubes as well as to effect a comparison between silver and gold nanocubes. We found that an increase in size, an increase in substrate refractive index, and a change of composition from silver to gold all lead to a red-shift of the plasmon resonance frequency. An unexpected finding is that for silver bipyramids, the dependence of the surface plasmon on size varies with the amount of truncation of the equatorial corners. Such results will play a crucial role in the design of plasmonic devices and the understanding of single particle surface-enhanced Raman spectroscopy.

ACKNOWLEDGMENTS

HRTEM work was performed in the EPIC facility of NUANCE Center at Northwestern University, supported by NSF-NSEC, NSF-MRSEC, Keck Foundation, the State of Illinois, and Northwestern University. This work was supported by the NSF (EEC-0647560, CHE-0414554, CHE-0911145, BES-0507036, DMR-0804088), AFOSR/DARPA Project BAA07-61 (FA9550-08-1-0221), AFOSR DURIP (FA9550-07-1-0526), DTRA JSTO (FA9550-06-1-0558), and the NSF MRSEC (DMR-0520513) at the Materials Research Center of Northwestern University.

REFERENCES

[1] A. J. Haes, L. Chang, W. L. Klein, and R. P. Van Duyne, *J. Am. chem. Soc.* **127**, 2264-2271 (2005).
[2] R. Elghanian, J. J. Storhoff, R. C. Mucic, R. L. Letsinger, and C. A. Mirkin, *Science* **277**, 1078-1081 (1997).
[3] H. A. Atwater, *Sci. Am.* **296**, 56-63 (2007).
[4] J. A. Dionne, L. A. Sweatlock, H. A. Atwater, and A. Polman, *Phys. rev. B* **73**, 035407 (2006).
[5] E. Ozbay, *Science*, **311**, 189-193, (2006).
[6] T. W. Ebbesen, C. Genet, and S. I. Bozhevolnyi, *Phys. Today* **61**, 44-50 (2008).
[7] R. Zia, J. A. Schuller, A. Chandran, and M. L. Brongersma, *Mater. Today* **9**, 20-27 (2006).
[8] P. L. Stiles, J. A. Dieringer, N. C. Shah, and R. P. Van Duyne, *Ann. Rev. Anal. Chem.* **1**, 601-626 (2008).
[9] J. Rodriguez-Fernandez, C. Novo, V. Myroshnychenko, A. M. Funston, A. Sanchez-Iglesias, I. Pastoriza-Santos, J. Perez-Juste, F. J. Garcia de Abajo, L. M. Liz-Marzan, and P. Mulvaney, *J. Phys. Chem. C* **113**, 18623-18631 (2009).
[10] J. M. McMahon, Y. Wang, L. J. Sherry, R. P. Van Duyne, L. D. Marks, S. K. Gray, and G. C. Schatz, *J. Phys. Chem. C* **113**, 2731-2735 (2009).
[11] Y. Wang, S. K. Eswaramoorthy, L. J. Sherry, J. A. Dieringer, J. P. Cadmen, G. C. Schatz, R. P. Van Duyne, and L. D. Marks, *Ultramicroscopy* **109**, 1110-1113 (2009).
[12] J. Zhang, S. Li, J. Wu, George C. Schatz, and Chad A. Mirkin, *Angew. Chem.* **121**, 7927-7931 (2009).
[13] Y. Sun and Y. Xia, *Science* **298**, 2176-2179 (2002).
[14] K. Sohn, F. Kim, K. C. Pradel, J. Wu, Y. Peng, F. Zhou, and J. Huang, *ACS Nano* **3**, 2191-2198 (2009).
[15] M. D. Malinsky, L. Kelly, G. C. Schatz, and R. P. Van Duyne, *J. Phys. Chem. B* **105**, 2343-2350 (2001).
[16] R. P. Shukla, A. Chowdhury, and P. D. Gupta, *Opt. Eng.* **33**, 1881-1884 (1994).
[17] L. J. Sherry, S.-H. Chang, G. C. Schatz, R. P. Van Duyne, B. J. Wiley, and Y. Xia, *Nano Letters* **5**, 2034-2038 (2005).
[18] G. C. Schatz (private communication).
[19] F. Zhou, Z.-Y. Li, Y. Liu, and Y. Xia, *J. Phys. Chem. C* **112**, 20233-20240 (2008).
[20] B. J. Wiley, Y. Xiong, Z.-Y. Li, Y. Yin, and Y. Xia, *Nano Letters* **6**, 765-768 (2006).